Research Square

Preprints are preliminary reports that have not undergone peer review.
They should not be considered conclusive, used to inform clinical practice,
or referenced by the media as validated information.

A novel high-order compact finite difference scheme in space and time for solving the generalized Rosenau-KdV-RLW equation

Yanling Chen
Ningxia Normal University
Xiaojia Yang
Ningxia Normal University
Lili Wu
Ningxia Normal University
Yingnan Qi
gysz9695@nxnu.edu.cn

Ningxia Normal University

Article

Keywords: Generalized Rosenau-KdV-RLW equation, Spatiotemporal fourth-order accuracy, Compact finite difference method, Conserved, Stable

Posted Date: April 21st, 2026

DOI: https://doi.org/10.21203/rs.3.rs-9200623/v1

License: This work is licensed under a Creative Commons Attribution 4.0 International License.
Read Full License

Additional Declarations: No competing interests reported.

A novel high-order compact finite difference scheme in space and time for solving the generalized Rosenau-KdV-RLW equation

Yanling Chen[1], Xiaojia Yang[1,2], Lili Wu[1], Yingnan Qi[1*]

1. *School of Mathematics and Computer Science, Ningxia Normal University, Guyuan 756000, China*

2. *Artificial Intelligence and Intelligent Medical Engineering Technology Research Center, Ningxia Normal University*

Abstract

In the high-accuracy numerical solution of the generalized Rosenau-KdV-RLW equation, the mismatch of the temporal and spatial accuracy orders often forces the calculation to adopt a fine grid to balance stability and accuracy. This not only significantly increases the computational cost but also intensifies the accumulation of rounding errors. To address this issue, this paper constructs a compact finite difference scheme with matched high-order spatiotemporal accuracy. For time discretization, the Crank-Nicolson scheme is adopted; Richardson extrapolation is then applied to elevate the temporal approximation accuracy to fourth order. Spatial discretization is carried out using the fourth-order compact finite difference method, which, while maintaining high spectral resolution, significantly reduces the width of the computational stencil and the storage requirements of the bandwidth matrix. We have established the stability and convergence theory of this scheme and proved the discrete conservation property; meanwhile, we have provided a strict analysis of the existence and uniqueness of the discrete solution. Numerical experiments demonstrate that the proposed scheme not only exhibits excellent validity and reliability but also maintains high-precision evolution on relatively coarse grids–thereby substantially improving numerical stability, conservation properties, and computational efficiency in long-term simulations.

Mathematics Subject Classification. $65M12, 65M06, 35Q75$.

Keywords: Generalized Rosenau-KdV-RLW equation; Spatiotemporal fourth-order accuracy; Compact finite difference method; Conserved; Stable

1. Introduction

The rich wave mechanics behaviors in nature are often effectively described by nonlinear equations. The Korteweg-de Vries (KdV) equation [5, 6, 11] characterizes unidirectional long waves under weak nonlinearity and weak dispersion conditions, and is seen in scenarios such as shallow water solitary waves and

*Corresponding author.

Email addresses : **m18295679926@163.com** (Y. Chen), **yangxj@nxnu.edu.cn** (X. Yang), **wll82003019@nxnu.edu.cn** (L. Wu), **gysz9695@nxnu.edu.cn** (Y. Qi).

plasma acoustic waves. The Regularized long-wave (RLW) equation [17, 18] is applicable to finite-amplitude unidirectional waves, such as medium-depth surface waves and plasma shock waves, but it has theoretical limitations in the presence of strong dissipation or bidirectional propagation. The Rosenau equation [20, 21] provides a dynamics modeling basis for dense discrete systems and is widely used in various solitary wave simulations. To further integrate multiple wave mechanisms, the Rosenau-KdV equation [7, 9, 19, 29] was proposed. Within a unified framework, it accounts for weak nonlinearity, dispersion, and dissipation effects and can describe cross-scale wave phenomena ranging from harbor waves to quantum ultracold atomic clouds. To address the deficiencies of traditional models in wave-wave interactions and boundary effects, a viscous correction term is introduced in this study to establish the generalized Rosenau-KdV-RLW system. This system simulates the propagation of shallow-water waves and internal waves in fluid mechanics, analyzes the behavior of light pulses in optical fibers in nonlinear optics, and is used to study stability and energy-transport processes in plasma physics. It has extensive theoretical and practical value. The generalized Rosenau-KdV-RLW equation is expressed as follows[1]

$$\frac{\partial u(x,t)}{\partial t}+\delta\frac{\partial^3 u(x,t)}{\partial x^2\partial t}+\nu\frac{\partial^5 u(x,t)}{\partial x^4\partial t}+\alpha\frac{\partial u(x,t)}{\partial x}+\theta\frac{\partial^3 u(x,t)}{\partial x^3}+\varepsilon\frac{\partial (u(x,t))^p}{\partial x}=0\ ,\ (x,t)\in\bar{\Omega}\times(0,T], \tag{1}$$

with the initial condition

$$u(x,\,0)=u_0(x), x\in\bar{\Omega}, \tag{2}$$

and the boundary condition

$$u(x,\ t)=\frac{\partial u(x,t)}{\partial x}=\frac{\partial^2 u(x,t)}{\partial x^2}=0\ ,\ x\in\partial\Omega, t\in(0,T]. \tag{3}$$

Let $u(x,t)$ denote the waveform, where x and t represent the spatial and temporal variables, respectively. The parameters α and ε correspond to the linear and nonlinear advection terms, while $p\geq 2$ is the exponent of the nonlinear power-law term. The coefficients θ, δ, and ν are associated with the KdV, RLW, and Rosenau terms, respectively. When $\delta=0$, the equation reduces to the Rosenau-KdV form; when $\theta=0$, it simplifies to the Rosenau-RLW form.

Due to the strong coupling between the nonlinear term and the dispersion effect in the Rosenau-KdV-RLW equation and the existence of high-order derivatives, obtaining an analytical solution is usually challenging. Therefore, numerical simulation has become an indispensable approach to studying the behavior of its solutions. In recent years, significant progress has been made in the research of numerical methods for such equations. For instance, Pan et al. [14–16] and Zhou et al. [26, 28] have respectively developed numerical methods for solving the Rosenau-RLW and Rosenau-KdV equations based on the Crank-Nicolson (C-N) scheme and the second-order central finite difference (FD) method. Özer [12, 13] constructed a variety of numerical schemes for the Rosenau-KdV-RLW equation based on the framework of Lie-Trotter and Strang operator splitting techniques, combined with the B-spline configuration point method and C-N scheme. Ak

et al. [3] adopted a numerical method based on hexagonal B-spline basis functions to solve the Rosenau-KdV equation. The motion of a single solitary wave, the interactions of two and three solitary waves, and the evolution of solitons under the initial conditions of Gaussian waves and undular bores were verified. Karta et al. [10] constructed a numerical solution scheme for the Rosenau-KdV equation based on the first-order Lie-Trotter and second-order Strang time splitting techniques, combined with the fourth-order Runge-Kutta (RK) scheme in the time direction and the quintic B-spline configuration method in the spatial direction. However, the overall accuracy of these methods is usually limited to second-order. Due to the strong numerical dissipation in the low-order format, on the one hand, it leads to amplitude attenuation and phase shift of the solitary wave; on the other hand, it is prone to excite non-physical oscillations in the steep-gradient region. Although grid refinement can offer limited improvements, it will significantly increase the computational cost. Therefore, constructing a numerical scheme that simultaneously possesses high accuracy and excellent stability is the fundamental approach to overcoming the aforementioned predicament and achieving high-fidelity, efficient simulation.

Based on the high-order FD scheme, many scholars have sought to solve the Rosenau-KdV-RLW equation and the Rosenau-KdV equation. Among them, the numerical formats constructed by Wang et al. [25], Ghiloufi et al. [8], and Apolinar-Fernandez et al. [4] all have a convergence order of $O(\tau^2 + h^4)$. Shallu et al. [22] numerically solved the Rosenau-KdV and Rosenau-RLW equations by using a configuration technique based on quintic B-splines and combining it with the strongly stable preservation type R-K method (SSP-RK). This scheme has third-order accuracy in time and second-order accuracy in space. Ahmat et al. [2] proposed a third-order weighted essentially oscillation-free (WENO) method for the generalized Rosenau-KdV-RLW equation. This method uses the third-order FD WENO reconstruction for the advective term in space and central FD discretization for the other terms. In terms of time, it uses the four-stage third-order SSP implicit-explicit RK method, thereby achieving the convergence accuracy of the third order in time and the fourth order in space. Although the existing high-precision formats each have their own advantages, their temporal and spatial accuracies often do not match. To achieve high-order spatial accuracy, fine time step size are often required to satisfy stability conditions, thereby significantly increasing computational resource consumption and reducing efficiency. This issue is particularly prominent in large-scale scientific computing and real-time engineering applications, and it has become a key bottleneck. Furthermore, an overly small time step can introduce significant rounding errors, distorting the proper solution and inducing non-physical oscillations. Therefore, it is vital to develop efficient and stable numerical methods for matching spatio-temporal convergence orders.

Ahmat et al. [1] adopted the fourth-order exponential time difference RK method to discretize the time direction. At the same time, the first and second derivatives of space were approximated using the fourth-order Padé scheme. For high-order derivative terms, this method converts fourth-order and third-

order derivatives into second-order and first-order forms by introducing intermediate variables, then applies the Padé formula again for discretization. However, this nested spatial discretization strategy is prone to accumulating errors during transmission, thereby deteriorating the overall numerical stability of the format. In this study, a high-order numerical scheme for spatio-temporal accuracy matching is proposed for the nonlinear Rosenau-KdV-RLW equation. In terms of spatial discretization, it integrates the fourth-order compact FD method, the Padé scheme, and the explicit combined compact FD scheme. In terms of time discretization, the C-N method was adopted, and the Richardson extrapolation method was used to achieve the fourth-order time accuracy. The core advantage of this scheme lies in its highly compact differential template design. By constructing high-order interpolation relationships between locally adjacent grid points, it can achieve fourth-order accuracy with only a few grid points, significantly improving computational efficiency while effectively suppressing numerical oscillation. Moreover, the proposed format still exhibits excellent stability and calculation accuracy at larger time steps.

The structure of this article is arranged as follows: Section 2 introduces the discretization methods of spatial derivatives and temporal derivatives. Section 3 conducts a theoretical analysis. Section 4 presents the numerical verification of the system. Finally, the section 5 summarizes the work of the entire text and proposes the future research directions.

2. The Construction of Higher-Order Compact FD Scheme

We employed a uniform grid in the spatial domain, where the space domain $\bar{\Omega} = [x_l, x_r]$ is divided into grid cells. The spatial step size is denoted as $h = (x_r - x_l)/N$ ($N \in \mathbb{Z}^+$). Let the time step be denoted as $\tau = T/M$, with $M \in \mathbb{Z}^+$ .The grid point is labeled as (x_i, t_n), and it holds that $x_i = x_l + ih$, $t_n = n\tau$, where $i = 0, 1, \cdots, N$ and $0 \le n \le M$. The numerical value at the point (x_i, t_n) is represented by u_i^n, while the exact solution is denoted as U_i^n. Let $V_h = \{u_i : i = 0, 1, \cdots, N\}$, $Z_h = \{u_i : u_0 = u_1 \cdots = u_{N-1} = u_N = 0\ , 0 \le i \le N\}$. For any grid function $u, v \in h$, the difference operator, the discrete inner product and the corresponding norm are defined as follows

$$\delta_x u_i = \frac{u_{i+1} - u_{i-1}}{2h}, \qquad \delta_x^2 u_i = \frac{u_{i+1} - 2u_i + u_{i-1}}{h^2}, \qquad \delta_t u^{n+\frac{1}{2}} = \frac{u^{n+1} - u^n}{\tau}, \quad u^{n+\frac{1}{2}} = \frac{u^{n+1} + u^n}{2},$$

$$\mathcal{A} = 1 + \frac{h^2}{12}\delta_x^2, \quad \mathcal{B} = 1 + \frac{h^2}{6}\delta_x^2, \quad (u, v) = \sum_{i=1}^{N-1} u_i v_i\, h, \quad \|u\| = \sqrt{(u, u)}, \quad \|u\|_H = \|u\|^2 + \|\mathcal{A}^{-1}\delta_x^2 u\|^2.$$

We define the fourth-order compact FD scheme for the second-order derivative as follows

$$\left(\frac{\partial^2 u}{\partial x^2}\right)_i = \mathcal{A}^{-1}\delta_x^2 u_i + O\left(h^4\right), \tag{4}$$

the fourth-order compact difference scheme for the fourth-order derivative is derived as follows

$$\left(\frac{\partial^4 u}{\partial x^4}\right)_i = \frac{\partial^2}{\partial x^2}\left(\frac{\partial^2 u}{\partial x^2}\right)_i = \mathcal{A}^{-1}\delta_x^2\left(\frac{\partial^2 u}{\partial x^2}\right)_i = \mathcal{A}^{-1}\delta_x^2\left(\mathcal{A}^{-1}\delta_x^2 u_i\right) = \mathcal{A}^{-2}\delta_x^2\delta_x^2 u_i + O\left(h^4\right), \tag{5}$$

the fourth-order Padé scheme for calculating first-order derivatives is defined as follows

$$\mathcal{B}\left(\frac{\partial u}{\partial x}\right)_i = \delta_x u_i + O\left(h^4\right), \tag{6}$$

i.e.,

$$\left(\frac{\partial u}{\partial x}\right)_i = (\mathcal{B})^{-1}\delta_x u_i + O\left(h^4\right), \tag{7}$$

Let D_1 be the Padé operator corresponding to the first-order derivative. The equation above can then be expressed as $\mathcal{B}D_1u_i = \delta_x u_i$, which implies that $D_1u_i = \mathcal{B}^{-1}\delta_x u_i$ and $\left(\frac{\partial u}{\partial x}\right)_0 = \left(\frac{\partial u}{\partial x}\right)_N = 0$, where $i = 1, 2, \ldots, N-1$, and the fourth-order explicit combined FD formulas for the second-order derivatives is derived through series expansion as follows

$$\left(\frac{\partial^2 u}{\partial x^2}\right)_i = 2\delta_x^2 u_i - \delta_x(D_1u_i)_i + O\left(h^4\right), \tag{8}$$

where $i = 1, 2, \cdots, N-1$,$\left(\frac{\partial^2 u}{\partial x^2}\right)_0 = \left(\frac{\partial^2 u}{\partial x^2}\right)_N = 0$. The values of $\left(\frac{\partial^2 u}{\partial x^2}\right)_{-1}$,$\left(\frac{\partial^2 u}{\partial x^2}\right)_{N+1}$,$\left(\frac{\partial u}{\partial x}\right)_{-1}$ and $\left(\frac{\partial u}{\partial x}\right)_{N+1}$ are calculated using the following fourth-order format

$$\begin{aligned}
\left(\frac{\partial^2 u}{\partial x^2}\right)_{-1} &= 5\left(\frac{\partial^2 u}{\partial x^2}\right)_0 - 10\left(\frac{\partial^2 u}{\partial x^2}\right)_1 + 10\left(\frac{\partial^2 u}{\partial x^2}\right)_2 - 5\left(\frac{\partial^2 u}{\partial x^2}\right)_3 + \left(\frac{\partial^2 u}{\partial x^2}\right)_4 + O\left(h^4\right), \\
\left(\frac{\partial^2 u}{\partial x^2}\right)_{N+1} &= 5\left(\frac{\partial^2 u}{\partial x^2}\right)_N - 10\left(\frac{\partial^2 u}{\partial x^2}\right)_{N-1} + 10\left(\frac{\partial^2 u}{\partial x^2}\right)_{N-2} - 5\left(\frac{\partial^2 u}{\partial x^2}\right)_{N-3} + \left(\frac{\partial^2 u}{\partial x^2}\right)_{N-4} + O\left(h^4\right),
\end{aligned} \tag{9}$$

$$\begin{aligned}
\left(\frac{\partial u}{\partial x}\right)_{-1} &= \frac{1}{h}\left(-\frac{3}{7}u_{-1} + \frac{41}{9}u_0 - \frac{25}{6}u_1 + \frac{17}{6}u_2 - \frac{19}{18}u_3 + \frac{1}{6}u_4\right) - \frac{1}{3}\left(\frac{\partial u}{\partial x}\right)_0 + O\left(h^4\right), \\
\left(\frac{\partial u}{\partial x}\right)_{N+1} &= \frac{1}{h}\left(\frac{11}{5}u_{N+1} - \frac{95}{18}u_N + \frac{11}{2}u_{N-1} - \frac{7}{2}u_{N-2} + \frac{23}{18}u_{N-3} - \frac{1}{5}u_{N-4}\right) + \frac{1}{3}\left(\frac{\partial u}{\partial x}\right)_N + O\left(h^4\right).
\end{aligned} \tag{10}$$

The third-order derivative of space is calculated using the following fourth-order format

$$\left(\frac{\partial^3 u}{\partial x^3}\right)_i = 2\delta_x^2 D_1 u_i - \delta_x \mathcal{A}^{-1}\delta_x^2 u_i + O\left(h^4\right), \tag{11}$$

where $i = 0, 1, 2, \cdots, N$. Let the fourth-order explicit combinatorial difference operator of the third-order derivative be D_3. From the above formula, it can be seen that $D_3u_i = 2\delta_x^2 D_1u_i - \delta_x\mathcal{A}^{-1}\delta_x^2 u_i$. For $\left(\frac{\partial^3 u}{\partial x^3}\right)_{-1}$ and $\left(\frac{\partial^3 u}{\partial x^3}\right)_{N+1}$, the following four-order format is adopted for calculation

$$\begin{aligned}
\left(\frac{\partial^3 u}{\partial x^3}\right)_{-1} = \frac{1}{h^2}&\left[\frac{12293}{2340}\left(\frac{\partial u}{\partial x}\right)_{-1} - \frac{18903}{1040}\left(\frac{\partial u}{\partial x}\right)_0 + \frac{2891}{104}\left(\frac{\partial u}{\partial x}\right)_1 - \frac{23941}{936}\left(\frac{\partial u}{\partial x}\right)_2\right] \\
&+ \frac{1}{h^2}\left[\frac{387}{26}\left(\frac{\partial u}{\partial x}\right)_3 - \frac{5063}{1040}\left(\frac{\partial u}{\partial x}\right)_4 + \frac{596}{120}\left(\frac{\partial u}{\partial x}\right)_5\right] - \frac{51}{52}\left(\frac{\partial^3 u}{\partial x^3}\right)_0 + O\left(h^4\right),
\end{aligned} \tag{12}$$

$$\begin{aligned}\left(\frac{\partial^3 u}{\partial x^3}\right)_{N+1} &= \frac{1}{h^2}\left[\frac{17599}{4680}\left(\frac{\partial u}{\partial x}\right)_{N+1} - \frac{17237}{1040}\left(\frac{\partial u}{\partial x}\right)_{N} + \frac{795}{26}\left(\frac{\partial u}{\partial x}\right)_{N-1} - \frac{28735}{936}\left(\frac{\partial u}{\partial x}\right)_{N-2}\right] \\ &+ \frac{1}{h^2}\left[\frac{1871}{104}\left(\frac{\partial u}{\partial x}\right)_{N-3} - \frac{6117}{1040}\left(\frac{\partial u}{\partial x}\right)_{N-4} + \frac{596}{120}\left(\frac{\partial u}{\partial x}\right)_{N-5}\right] + \frac{51}{52}\left(\frac{\partial^3 u}{\partial x^3}\right)_N + O\left(h^4\right).\end{aligned} \tag{13}$$

The Sobolev space is defined as follows [25]

$$H^k(\Omega) = \left\{u(x) : \int_\Omega \left(u^{(j)}\right)^2 dx < +\infty,\ j = 0, 1, 2, \cdots, k-1, k\right\},$$

$$H_0^k(\Omega) = \left\{u(x) \in H^k(\Omega) : \left.\frac{\partial^i u}{\partial x^i}\right| \partial\Omega = 0,\ i = 0, 1, 2, \cdots, k-1\right\}.$$

where $u^{(j)}$ is the j^{th} order derivative. The Rosenau-KdV equation satisfies the following conservation laws

$$Q(t) = \int_{x_l}^{x_r} u(x,t)dx = \int_{x_l}^{x_r} u(x,0)dx = \int_{x_l}^{x_r} u_0(x)dx = Q(0), \tag{14}$$

$$\begin{aligned}E(t) &= \int_{x_l}^{x_r}\left(u(x,t)^2 + \left(\frac{\partial^2 u(x,t)}{\partial x^2}\right)^2\right)dx = \|u(x,t)\|^2 + \left\|\frac{\partial^2 u(x,t)}{\partial x^2}\right\|^2 \\ &= \|u_0(x)\|^2 + \left\|\frac{\partial^2 u_0(x)}{\partial x^2}\right\| = E(0),\end{aligned} \tag{15}$$

among them $u_0(x) \in H_0^k(\Omega)$, $Q(0)$ and $E(0)$ are constants related to the initial values.

2.1. Spatial Derivative Discretization

Firstly, to facilitate the establishment of the numerical result of Eqs. (1) - (3), rewrite Eq. (1) as follows

$$\frac{\partial u(x,t)}{\partial t} + \delta\frac{\partial^3 u(x,t)}{\partial x^2 \partial t} + \nu\frac{\partial^5 u(x,t)}{\partial x^4 \partial t} + f[u(x,t)] = 0, \tag{16}$$

where

$$f[u(x,t)] = \alpha\frac{\partial u(x,t)}{\partial x} + \theta\frac{\partial^3 u(x,t)}{\partial x^3} + \varepsilon\frac{\partial [u(x,t)]^p}{\partial x}. \tag{17}$$

Evaluating Eqs. (16) and (17) at the grid point x_i, we approximate the second- and fourth-order spatial derivatives via the fourth-order compact FD schemes (4) and (5), respectively; the first- and third-order spatial derivatives in Eq. (17) are discretized using the fourth-order Padé scheme (6) and the fourth-order combinatorial FD formula (11), respectively. This yields

$$\left(\frac{\partial u(x,t)}{\partial t}\right)_i + \delta\mathcal{A}^{-1}\delta_x^2\left(\frac{\partial u(x,t)}{\partial t}\right)_i + \nu\mathcal{A}^{-2}\delta_x^2\delta_x^2\left(\frac{\partial u(x,t)}{\partial t}\right)_i = -f(u_i). \tag{18}$$

where $f(u_i) = \alpha\mathcal{B}^{-1}\delta_x u_i + \theta\left(2\delta_x^2\mathcal{B}^{-1}\delta_x u_i - \delta_x\mathcal{A}^{-1}\delta_x^2 u_i\right) + \varepsilon\mathcal{B}^{-1}\delta_x(u^p)_i$, $i = 1, 2, \cdots, N-1$.

2.2. Time Derivative Discretization

Considering the values of Eq. (18) at the $\left(n+\frac{1}{2}\right)-th$ layer, we discretize the time derivative using the C-N scheme, resulting in

$$\delta_t u_i^{n+\frac{1}{2}} + \delta \mathcal{A}^{-1}\delta_x^2\left(\delta_t u_i^{n+\frac{1}{2}}\right) + \nu\mathcal{A}^{-2}\delta_x^2\delta_x^2\left(\delta_t u_i^{n+\frac{1}{2}}\right) = -f\left(u_i^{n+\frac{1}{2}}\right). \tag{19}$$

Multiplying both sides of the equation by the operator $\mathcal{A}^2$ and substituting the definitions of $\mathcal{A}$ and $\delta_t u_i^{n+\frac{1}{2}}$, we obtain

$$\begin{aligned}
&\frac{h^4+12\delta h^2+144\nu}{144h^4}\left(u_{i+2}^{n+1}+u_{i-2}^{n+1}\right)+\left(\frac{5}{36}+\frac{2\delta h^2-12\nu}{3h^4}\right)\left(u_{i+1}^{n+1}+u_{i-1}^{n+1}\right)+\left(\frac{17}{24}+\frac{72\nu-18\delta h^2}{12h^4}\right)u_i^{n+1}\\
&=-\frac{1}{144}\left(\frac{f\left(u_{i+2}^{n+1}\right)+f\left(u_{i+2}^{n}\right)+f\left(u_{i-2}^{n+1}\right)+f\left(u_{i-2}^{n}\right)}{2}\right)-\frac{5}{36}\left(\frac{f\left(u_{i+1}^{n+1}\right)+f\left(u_{i+1}^{n}\right)+f\left(u_{i-1}^{n+1}\right)+f\left(u_{i-1}^{n}\right)}{2}\right)\\
&\quad-\frac{1}{24}\left(\frac{f\left(u_i^{n+1}\right)+f\left(u_i^{n}\right)}{2}\right)+\left(\frac{17}{24\tau}+\frac{72\nu-18\delta h^2}{12\tau h^2}\right)u_i^n+\left(\frac{5}{36\tau}+\frac{2\delta h^2-12\nu}{3\tau h^4}\right)\left(u_{i+1}^n+u_{i-1}^n\right)\\
&\quad+\frac{h^4+12\delta h^2+144\nu}{144\tau h^4}\left(u_{i+2}^n+u_{i-2}^n\right)
\end{aligned} \tag{20}$$

where $i=1,2,\cdots,N-1$, the values of u_{-1} and u_{N+1} is solved by Eq. (9). The above equation represents a high-order compact FD scheme that achieves second-order accuracy in time and fourth-order accuracy in space for solving Eqs. (1)-(3). It is named the HOC-24 scheme. To achieve spatio-temporal precision matching, we introduce the following Richardson extrapolation technique on the basis of the above format

$$\widehat{u}_i^n(\tau)=\frac{32}{21}u_i^{4n}\left(\frac{\tau}{4}\right)-\frac{12}{21}u_i^{2n}\left(\frac{\tau}{2}\right)+\frac{1}{21}u_i^n(\tau), 1\le n\le M. \tag{21}$$

Therefore, Eqs. (20) and (21) together form a fourth-order consistent FD scheme in both time and space for solving Eqs. (1)-(3). Its spatial discretization only depends on five adjacent grid points, which is a typical compactness feature. This method is named the HOC-44 scheme.

3. Theoretical Analysis

Next,we consider some properties of the HOC-24 and HOC-44 schemes for the Rosenau-KdV equation when $\delta=0,\ v=\alpha=\theta=1,\ \varepsilon=\frac{1}{2}$ and $p=2$ in Eq. (1). For the Rosenau-KdV equation under these parameters, to ensure the conservation property of the format, the nonlinear terms are handled as follows when constructing the HOC-24 and HOC-44 schemes

$$\frac{1}{2}\left(\frac{\partial u^2}{\partial x}\right)=\frac{1}{3}\left(\frac{\partial u^2}{\partial x}\right)+\frac{1}{3}u\frac{\partial u}{\partial x}, \tag{22}$$

thus, the HOC-24 format for solving the Rosenau-KdV equation becomes the following form

$$\delta_t u_i^{n+\frac{1}{2}}+\mathcal{A}^{-2}\delta_x^2\delta_x^2\delta_t u_i^{n+\frac{1}{2}}+D_1 u_i^{n+\frac{1}{2}}+D_3 u_i^{n+\frac{1}{2}}+\frac{1}{3}D_1(u^2)_i^{n+\frac{1}{2}}+\frac{1}{3}u^{n+\frac{1}{2}}(D_1 u_i^{n+\frac{1}{2}})=0. \tag{23}$$

First, we present several preparatory lemmas.

Lemma 1. *For $\forall u, v \in Z_h$, the following holds*

$$\sum_{i=1}^{N-1} \mathcal{A}u_i = \sum_{i=1}^{N-1} u_i, \qquad \sum_{i=1}^{N-1} \mathcal{A}^{-1}u_i = \sum_{i=1}^{N-1} u_i, \qquad \sum_{i=1}^{N-1} \delta_x^2 u_i = 0,$$
$$\sum_{i=1}^{N-1} \mathcal{B}u_i = \sum_{i=1}^{N-1} u_i, \qquad \sum_{i=1}^{N-1} \mathcal{B}^{-1}u_i = \sum_{i=1}^{N-1} u_i, \qquad \sum_{i=1}^{N-1} \delta_x u_i = 0.$$

Lemma 2. *For $\forall u, v \in Z_h$, the following holds*

$$(\mathcal{A}u, v) = (u, \mathcal{A}v), \qquad \left(\mathcal{A}^{-1}u, v\right) = \left(u, \mathcal{A}^{-1}v\right), \qquad (\delta_x u, v) = -(u, \delta_x v),$$
$$(\mathcal{B}u, v) = (u, \mathcal{B}v), \qquad \left(\mathcal{B}^{-1}u, v\right) = \left(u, \mathcal{B}^{-1}v\right), \qquad \left(\delta_x^2 u, v\right) = \left(u, \delta_x^2 v\right).$$

Lemma 3. *For $\forall u, v \in Z_h$, it holds that*

$$(D_1 u, v) = -(u, Dv),$$

and in particular, we have

$$(D_1 u, u) = 0.$$

The proofs of Lemmas 1 to 3 can be found in detail in Ref. [23].

Lemma 4. *For $\forall u, v \in Z_h$, it holds that*

$$(u, \mathrm{D}_3 u) = 0.$$

Proof. Because

$$D_3{}^T = \left(2\delta_x^2 D_1 - \delta_x \mathcal{A}^{-1}\delta_x^2\right)^T = 2D_1{}^T\left(\delta_x^2\right)^T - \left(\delta_x^2\right)^T\left(\mathcal{A}^{-1}\right)^T(\delta_x)^T.$$

It can be derived from Lemmas 2 and 3

$$D_3{}^T = -2D_1\delta_x^2 + \delta_x^2\mathcal{A}^{-1}\delta_x = -D_3.$$

Then the operator D_3 is merely symmetric, that is

$$(D_3 u, u) = -(u, D_3 u).$$

In particular,

$$(u, D_3 u) = 0.$$

Thus, the proof is complete. □

Lemma 5. *For $\forall u \in Z_h$, it follows that*

$$\sum_{i=1}^{N-1} D_3 u_i = 0.$$

3.1. The Conservation of HOC-24 and HOC-44 Schemes

Theorem 1. *The HOC-24 scheme and the HOC-44 scheme for solving the Rosenau-KdV equation both satisfy the discrete conservation of mass law*

$$Q^n = Q^{n+1}. \tag{24}$$

for any $n \geq 0$,

$$Q^n = h\sum_{i=1}^{N-1} u^n = (u^n, I)\,. \tag{25}$$

Proof. The inner product of I with the Eq. (23) yields the result

$$\begin{aligned}&\left(I, \delta_t u^{n+\frac{1}{2}}\right) + \left(I, \mathcal{A}^{-2}\delta_x^2\delta_x^2\delta_t u^{n+\frac{1}{2}}\right) + \left(I, D_1 u^{n+\frac{1}{2}}\right) + \left(I, D_3 u^{n+\frac{1}{2}}\right)\\ &+ \left(I, \frac{1}{3}D_1\left(u^2\right)^{n+\frac{1}{2}}\right) + \left(I, \frac{1}{3}u^{n+\frac{1}{2}}(D_1 u^{n+\frac{1}{2}})\right) = 0.\end{aligned} \tag{26}$$

By analyzing each term of the above equation, we obtain

$$\left(I, \delta_t u^{n+\frac{1}{2}}\right) = \left(I, \frac{u_i^{n+1} - u_i^n}{\tau}\right) = \frac{Q^{n+1} - Q^n}{\tau}.$$

Based on Lemma 1, it follows that

$$\left(I, \mathcal{A}^{-2}\delta_x^2\delta_x^2\delta_t u^{n+\frac{1}{2}}\right) = 0, \quad \left(I, D_1 u^{n+\frac{1}{2}}\right) = 0, \quad \left(I, \frac{1}{3}D_1\left(u^2\right)^{n+\frac{1}{2}} + \frac{1}{3}u^{n+\frac{1}{2}}D_1 u^{n+\frac{1}{2}}\right) = 0.$$

It can be inferred from Lemma 5 that

$$\left(I, D_3 u^{n+\frac{1}{2}}\right) = 0.$$

Based on the above estimates, the Eq. (26) is simplified to

$$\frac{Q^{n+1} - Q^n}{\tau} = 0, \quad i.e., \quad Q^{n+1} = Q^n.$$

Next, to prove the mass conservation of the HOC-44 scheme, we take the inner product of Eq. (21) with I. By utilizing the definition of Q^n, we obtain

$$\begin{aligned}Q\left(\widehat{u}^n(\tau)\right) &= Q\left(\frac{32}{21}u^{4n}\left(\frac{\tau}{4}\right) - \frac{12}{21}u^{2n}\left(\frac{\tau}{2}\right) + \frac{1}{21}u^n(\tau)\right)\\ &= \frac{32}{21}Q\left(u^{4n}\left(\frac{\tau}{4}\right)\right) - \frac{12}{21}Q\left(u^{2n}\left(\frac{\tau}{2}\right)\right) + \frac{1}{21}Q\left(u^n(\tau)\right)\\ &= \left(\frac{32}{21} - \frac{12}{21} + \frac{1}{21}\right)Q^0 = Q^0.\end{aligned} \tag{27}$$

From the arbitrary nature of n, it follows that Q^{n+1}=Q^n. This proof is complete. □

Theorem 2. *The HOC-24 scheme satisfies the discrete energy conservation law*

$$E^{n+1} = E^n, \tag{28}$$

for any $n \geq 0$, *where*

$$E^n = \|u^n\|^2 + \|\mathcal{A}^{-1}\delta_x^2 u^n\|^2. \tag{29}$$

Proof. Taking the inner product of Eq. (23) with $u^{n+\frac{1}{2}}$ yields

$$\begin{aligned}\left(u^{n+\frac{1}{2}},\delta_t u^{n+\frac{1}{2}}\right)+\left(u^{n+\frac{1}{2}},\mathcal{A}^{-2}\delta_x^2\delta_x^2\delta_t u^{n+\frac{1}{2}}\right)+\left(u^{n+\frac{1}{2}},D_1u^{n+\frac{1}{2}}+D_3u^{n+\frac{1}{2}}\right)\\+\left(u^{n+\frac{1}{2}},\frac{1}{3}D_1\left(u^{n+\frac{1}{2}}\right)^2\right)+\frac{1}{3}\left(u^{n+\frac{1}{2}},u^{n+\frac{1}{2}}D_1u^{n+\frac{1}{2}}\right),\\+\left(u^{n+\frac{1}{2}},\frac{1}{3}D_1\left(u^{n+\frac{1}{2}}\right)^2\right)+\frac{1}{3}\left(u^{n+\frac{1}{2}},u^{n+\frac{1}{2}}D_1u^{n+\frac{1}{2}}\right),\end{aligned}\tag{30}$$

the first term on the left side of the Eq. (30) is

$$\left(u^{n+\frac{1}{2}},\delta_t u^{n+\frac{1}{2}}\right)=\frac{1}{2\tau}\left(\left\|u^{n+1}\right\|^2-\left\|u^n\right\|^2\right),\tag{31}$$

according to Lemma 2, the second term on the left side of Eq. (30) is

$$\left(u^{n+\frac{1}{2}},\mathcal{A}^{-2}\delta_x^2\delta_x^2\delta_t u^{n+\frac{1}{2}}\right)=\left(\mathcal{A}^{-1}\delta_x^2u^{n+\frac{1}{2}},\mathcal{A}^{-1}\delta_x^2\delta_t u^{n+\frac{1}{2}}\right)=\frac{1}{2\tau}\left(\left\|\mathcal{A}^{-1}\delta_x^2u^{n+1}\right\|^2-\left\|\mathcal{A}^{-1}\delta_x^2u^n\right\|^2\right),\tag{32}$$

according to Lemmas 3 and 4, the third term on the left-hand side of Eq. (30) is

$$\left(u^{n+\frac{1}{2}},D_1u^{n+\frac{1}{2}}+D_3u^{n+\frac{1}{2}}\right)=0,\tag{33}$$

from Lemma 3, the nonlinear term in Eq. (30) can be expressed as follows

$$\begin{aligned}&\left(u^{n+\frac{1}{2}},\frac{1}{3}D_1\left(u^{n+\frac{1}{2}}\right)^2\right)+\frac{1}{3}\left(u^{n+\frac{1}{2}},u^{n+\frac{1}{2}}D_1u^{n+\frac{1}{2}}\right)\\&=-\frac{1}{3}\left(D_1u^{n+\frac{1}{2}},\left(u^{n+\frac{1}{2}}\right)^2\right)+\frac{1}{3}\left(u^{n+\frac{1}{2}},u^{n+\frac{1}{2}}D_1u^{n+\frac{1}{2}}\right)\\&=-\frac{1}{3}\sum_{i=1}^{N-1}\left(D_1u_i^{n+\frac{1}{2}}\right)\left(u_i^{n+\frac{1}{2}}\right)^2+\frac{1}{3}\sum_{i=1}^{N-1}u_i^{n+\frac{1}{2}}u_i^{n+\frac{1}{2}}D_1u_i^{n+\frac{1}{2}}\\&=0.\end{aligned}\tag{34}$$

Therefore, we obtain

$$\frac{1}{2\tau}\left(\left\|u^{n+1}\right\|^2+\left\|\mathcal{A}^{-1}\delta_x^2u^{n+1}\right\|^2\right)=\frac{1}{2\tau}\left(\left\|u^n\right\|^2+\left\|\mathcal{A}^{-1}\delta_x^2u^n\right\|^2\right),\tag{35}$$

that is $E^{n+1}=E^n$. The proof of the theorem is complete. □

3.2. The Stability of HOC-24 and HOC-44 Schemes

Next, we need to prove the stability of the HOC-24 and HOC-44 schemes.

Lemma 6. *Supposing that $U_0(x)\in H_0^2(\Omega)$, the exact solution U of the Rosenau-KdV Eqs. (1)-(3) satisfies*

$$\|U\|\le C,\quad \left\|\frac{\partial^2U}{\partial x^2}\right\|\le C,\quad \|U\|_{L_\infty}\le C.\tag{36}$$

Proof. It follows from Eq. (15) that

$$E(t) = \|U\|^2 + \left\|\frac{\partial^2 U}{\partial x^2}\right\|^2 = \|U_0(x)\|^2 + \left\|\frac{\partial^2 U_0(x)}{\partial x^2}\right\|^2 = E(0) = C. \tag{37}$$

Clearly, we have

$$\|U\| \leq C \quad \text{and} \quad \left\|\frac{\partial^2 U}{\partial x^2}\right\| \leq C. \tag{38}$$

By applying Sobolev's inequality, we can conclude that $\|U\|_{L_\infty} \leq C$.

The proof of this lemma is complete. □

Lemma 7. *Supposing that $u_0(x) \in H_0^2(\Omega)$, the numerical solution u of the scheme (23) satisfies*

$$\|u^n\| \leq C, \quad \left\|\delta_x^2 u^n\right\|^2 \leq C, \quad \|u^n\|_{L_\infty} \leq C. \tag{39}$$

Proof. It follows from Eq. (29) that

$$E^n = \|u^n\|^2 + \left\|\delta_x^2 \mathcal{A}^{-1} u^n\right\|^2 = E^0 = C. \tag{40}$$

Thus, we have

$$\|u^n\|^2 \leq C, \qquad \left\|\delta_x^2 \mathcal{A}^{-1} u^n\right\|^2 \leq C. \tag{41}$$

By Lemma 1, it is established that

$$\left\|\delta_x^2 \mathcal{A}^{-1} u^n\right\|^2 = \left\|\delta_x^2 u^n\right\| \leq C. \tag{42}$$

By the discrete Sobolev's inequality, we obtain

$$\|u^n\|_{L_\infty} \leq C. \tag{43}$$

The proof of this lemma is complete. □

According to Lemmas 6 and 7, we can establish the following theorem on unconditional stability.

Theorem 3. *The HOC-24 scheme exhibits unconditional stability.*

The stability conclusion of the HOC-44 scheme is as follows:

Theorem 4. *The HOC-44 scheme exhibit stability in accordance with the Lax-Richtmyer framework.*

Proof. From the HOC-24 scheme (23) satisfying the discrete energy conservation property, it can be obtained that

$$\left\|u^{4n}\left(\frac{\tau}{4}\right)\right\|_H = E(0), \left\|u^{2n}\left(\frac{\tau}{2}\right)\right\|_H = E(0), \|u^n(\tau)\|_H = E(0). \tag{44}$$

Taking the norm of Eq. (21), we derive

$$\begin{aligned} \|\widehat{u}^n(\tau)\|_H &= \left\|\frac{32}{21}u^{4n}\left(\frac{\tau}{4}\right) - \frac{12}{21}u^{2n}\left(\frac{\tau}{2}\right) + \frac{1}{21}u^n(\tau)\right\|_H \\ &\leq \frac{32}{21}\left\|u^{4n}\left(\frac{\tau}{4}\right)\right\|_H + \frac{12}{21}\left\|u^{2n}\left(\frac{\tau}{2}\right)\right\|_H + \frac{1}{21}\|u^n(\tau)\|_H. \end{aligned} \tag{45}$$

Substituting Eq. (44) into the above formula yields

$$\left\|\widehat{u}^{n}(\tau)\right\|_{H} \leq \frac{15}{7} E(0). \tag{46}$$

$E(0)$ is a constant that remains independent of n, indicating that the solution does not exhibit exponential growth over time. Consequently, this formulation is stable according to the Lax-Richtmyer definition.

The proof of this theorem is complete. □

3.3. The Existence and Uniqueness of Solutions

Lemma 8. (**The corollary of Brouwer's fixed point theorem**) *Let H be a finite-dimensional Hilbert space with the inner product $(\cdot,\cdot)$, $\|\cdot\|$ the ssiciated norm, $g: H \to H$ be continuous. Assume moreover that*

$$\exists a>0, \quad \forall z \in H, \quad \|z\|=a, \quad (g(z), z)>0. \tag{47}$$

Then there exists $z^{*} \in H$ such that $g(z^{*})=0$ and $\|z^{*}\| \leq a$.

Theorem 5. *For the given initial value u^{n}, the solution u^{n+1} of the HOC-24 scheme exists at time t_{n+1}.*

Proof. Let $v=u^{n+1}$, and define the mapping $g(v)$ as

$$g(v)=\frac{v-u^{n}}{\tau}+\mathcal{A}^{-2}\delta_{x}^{2}\delta_{x}^{2}\left(\frac{v-u^{n}}{\tau}\right)+\mathcal{L}\left(\frac{v+u^{n}}{2}\right)+Q\left(\frac{v+u^{n}}{2}\right), \tag{48}$$

here, $\mathcal{L}$ represents the discrete operators of the linear first-order and third-order derivative terms. $Q(w)$ represents the discrete operator of the nonlinear term $\frac{1}{3}\frac{\partial\left(w^{2}\right)}{\partial x}+\frac{1}{3} w \frac{\partial w}{\partial x}$. Let $\bar{v}=\frac{v+u^{n}}{2}$. By taking the inner product of v and $g(v)$, we obtain

$$(g(v), \bar{v})=\left(\frac{v-u^{n}}{\tau}, \bar{v}\right)+\left(\mathcal{A}^{-2}\delta_{x}^{2}\delta_{x}^{2}\left(\frac{v-u^{n}}{\tau}\right), \bar{v}\right)+(\mathcal{L}(\bar{v}), \bar{v})+(Q(\bar{v}), \bar{v}). \tag{49}$$

From Lemmas 3 and 4, we obtain

$$(\mathcal{L}(\bar{v}), \bar{v})=0 \quad \text{and} \quad (Q(\bar{v}), \bar{v})=0. \tag{50}$$

From Lemma 2, it can be inferred that

$$\left(\mathcal{A}^{-2}\delta_{x}^{2}\delta_{x}^{2}\left(\frac{v-u^{n}}{\tau}\right), \bar{v}\right)=\frac{1}{2\tau}\left(\left\|\mathcal{A}^{-1}\delta_{x}^{2} v\right\|-\left\|\mathcal{A}^{-1}\delta_{x}^{2} u^{n}\right\|\right). \tag{51}$$

Consequently,

$$(g(v), \bar{v})=\frac{1}{2\tau}\left(\|v\|-\|u^{n}\|\right)+\frac{1}{2\tau}\left(\left\|\mathcal{A}^{-1}\delta_{x}^{2} v\right\|-\left\|\mathcal{A}^{-1}\delta_{x}^{2} u^{n}\right\|\right)=\frac{1}{2\tau}\left(\|v\|_{H}^{2}-\|u^{n}\|_{H}^{2}\right). \tag{52}$$

Consider a sphere with a radius of a_{m}, where $a=\|u^{n}\|_{H}+\varepsilon$ and $\forall \varepsilon>0$. For any vector v that satisfies $\|v\|_{H}=a$, it is obvious that $\|v\|_{H}>\|u^{n}\|_{H}$. Substituting this into the above equation yields

$$(g(v), \bar{v})=\frac{1}{2\tau}\left(a^{2}-\|u^{n}\|_{H}^{2}\right)>0. \tag{53}$$

By Lemma 8, within the sphere defined by $\|v\|_H \leq \mathrm{a}$, there exists a value v^* such that $g(v^*) = 0$. Consequently, u^{n+1} is guaranteed to exist.

We have completed the proof of this theorem. □

Theorem 6. *When the value of τ is sufficiently small, the solution of the HOC-24 scheme is unique.*

Proof. At time t_{n+1}, there exist two solutions u^{n+1} and v^{n+1}. By substituting u^{n+1} and v^{n+1} into Eq. (23) respectively and then subtracting the results, we define $w^{n+1} = u^{n+1} - v^{n+1}$. Consequently, we obtain result

$$\frac{w^{n+1}}{\tau} + \mathcal{A}^{-2}\delta_x^2\delta_x^2\frac{w^{n+1}}{\tau} + \mathcal{L}\frac{w^{n+1}}{2} + \left[Q\left(\frac{u^{n+1}+u^n}{2}\right) - Q\left(\frac{v^{n+1}+u^n}{2}\right)\right] = 0. \tag{54}$$

Let $\bar{u} = \frac{u^{n+1}+u^n}{2}$ and $\bar{v} = \frac{v^{n+1}+v^n}{2}$. Then, we have $\bar{u} - \bar{v} = \frac{w^{n+1}}{2}$. By substituting this notation into the preceding equation and taking the inner product with w^{n+1}, we obtain

$$\frac{1}{\tau}\left\|w^{n+1}\right\|_H^2 + \left(\mathcal{L}\frac{w^{n+1}}{2}, w^{n+1}\right) + \left(Q(\bar{u}) - Q(\bar{v}), w^{n+1}\right) = 0. \tag{55}$$

From Lemmas 3 and 4, it can be inferred that

$$\left(\mathcal{L}\frac{w^{n+1}}{2}, w^{n+1}\right) = 0, \tag{56}$$

Consequently, Eq. (55) can be simplified to yield

$$\frac{1}{\tau}\left\|w^{n+1}\right\|_H^2 = -\left(Q(\bar{u}) - Q(\bar{v}), w^{n+1}\right). \tag{57}$$

Because

$$Q(\bar{u}) - Q(\bar{v}) = \frac{1}{3}\left[\frac{\partial(\bar{u})^2}{\partial x} - \frac{\partial(\bar{v})^2}{\partial x}\right] + \frac{1}{3}\left(\bar{u}\frac{\partial\bar{u}}{\partial x} - \bar{v}\frac{\partial\bar{v}}{\partial x}\right), \tag{58}$$

and by virtue of the Sobolev embedding theorem, as well as Theorems 2 and 4, there exists a constant C such that

$$\|Q(\bar{u}) - Q(\bar{v})\| \leq C\max\left\{\|u^n\|_H, \left\|u^{n+1}\right\|_H, \left\|v^{n+1}\right\|_H\right\}\left\|w^{n+1}\right\|_H. \tag{59}$$

Then

$$\left\|\left(Q(\bar{v}) - Q(\bar{u}), w^{n+1}\right)\right\| \leq \|Q(\bar{v}) - Q(\bar{u})\| \cdot \left\|w^{n+1}\right\| \leq C\left\|w^{n+1}\right\|_H^2, \tag{60}$$

substituting Eq. (60) into (57) yields

$$\frac{1}{\tau}\left\|w^{n+1}\right\|_H^2 \leq C\left\|w^{n+1}\right\|_H^2, \tag{61}$$

that is

$$(1 - C\tau)\left\|w^{n+1}\right\|_H^2 \leq 0. \tag{62}$$

Therefore, when $\tau < \frac{1}{C}$, $u^{n+1} = v^{n+1}$, meaning that the discrete solution u^{n+1} is unique.

This proof is completed. □

Theorem 7. *The solution $U^n(\tau)$ of the HOC-44 scheme exists and is unique.*

Proof. According to Theorem 6, it can be concluded that $u^{4n}\left(\frac{\tau}{4}\right)$, $u^{2n}\left(\frac{\tau}{2}\right)$, and $u^n(\tau)$ exist and are unique. Furthermore, $\widehat{u}^n(\tau)$ is a linear combination of these functions. Based on the closure property and monotonicity of linear operations within a linear space, we can deduce that $\widehat{u}^n(\tau)$ also exists and is unique. □

3.4. The Convergence of HOC-24 and HOC-44 Schemes

Theorem 8. *Let $\mathrm{e}^n = U^n - u^n$, where U^n represents the exact solution and u^n denotes the numerical solution in the HOC-24 scheme. For any fixed $T > 0$, there exists a constant C independent of τ and h, such that*

$$\|e^n\|_H \leq C\left(\tau^2 + h^4\right),$$

for sufficiently small τ and h.

Proof. From the derivation process, it is established that the truncation error satisfies $R_i^n = O\left(\tau^2 + h^4\right)$. Consequently, there exists a constant C_1 such that $\|R^n\| \leq C_1\left(\tau^2 + h^4\right)$. Substituting the numerical error e^n into Eq. (23) yields

$$\frac{e^{n+1}-e^n}{\tau} + \mathcal{A}^{-2}\delta_x^2\delta_x^2\frac{e^{n+1}-e^n}{\tau} + \mathcal{L}\left(\frac{e^{n+1}+e^n}{2}\right) + \left[Q\left(u^{n+\frac{1}{2}}\right) - Q\left(U^{n+\frac{1}{2}}\right)\right] = R^n.$$

Taking the inner product of the aforementioned equation with $\frac{e^{n+1}+e^n}{2}$, we obtain

$$\begin{aligned}&\left(\frac{e^{n+1}-e^n}{\tau} + \mathcal{A}^{-2}\delta_x^2\delta_x^2\frac{e^{n+1}-e^n}{\tau}, \frac{e^{n+1}+e^n}{2}\right) + \left(\mathcal{L}\left(\frac{e^{n+1}+e^n}{2}\right), \frac{e^{n+1}+e^n}{2}\right)\\ &+ \left(Q\left(u^{n+\frac{1}{2}}\right) - Q\left(U^{n+\frac{1}{2}}\right), \frac{e^{n+1}+e^n}{2}\right) = \left(R^n, \frac{e^{n+1}+e^n}{2}\right).\end{aligned} \tag{63}$$

Among them,

$$\left(\frac{e^{n+1}-e^n}{\tau} + \mathcal{A}^{-2}\delta_x^2\delta_x^2\frac{e^{n+1}-e^n}{\tau}, \frac{e^{n+1}+e^n}{2}\right) \leq \frac{1}{2\tau}\left(\left\|e^{n+1}\right\|_H^2 - \|e^n\|_H^2\right), \tag{64}$$

$$\left(\mathcal{L}\left(\frac{e^{n+1}+e^n}{2}\right), \frac{e^{n+1}+e^n}{2}\right) = 0, \tag{65}$$

$$\left|\left(Q\left(u^{n+\frac{1}{2}}\right) - Q\left(U^{n+\frac{1}{2}}\right), \frac{e^{n+1}+e^n}{2}\right)\right| \leq C_2\left\|\frac{e^{n+1}+e^n}{2}\right\|_H^2, \tag{66}$$

$$\left(R^n, \frac{e^{n+1}+e^n}{2}\right) \leq \|R^n\|\left\|\frac{e^{n+1}+e^n}{2}\right\| \leq \frac{1}{2}\|R^n\|^2 + \frac{1}{2}\left\|\frac{e^{n+1}+e^n}{2}\right\|^2 \leq \frac{1}{2}\|R^n\|^2 + \frac{1}{2}\left\|\frac{e^{n+1}+e^n}{2}\right\|_H^2. \tag{67}$$

Substituting the Eqs. (64)-(67) into (63) yields

$$\begin{aligned}\frac{1}{2\tau}\left(\|e^{n+1}\|_H^2 - \|e^n\|_H^2\right) &\leq C_2\left\|\frac{e^{n+1}+e^n}{2}\right\|_H^2 + \frac{1}{2}\left\|\frac{e^{n+1}+e^n}{2}\right\|_H^2 + \frac{1}{2}\|R^n\|^2\\ &\leq \frac{1}{2}C_2\left(\|e^{n+1}\|_H^2 + \|e^n\|_H^2\right) + \frac{1}{4}\left(\|e^{n+1}\|_H^2 + \|e^n\|_H^2\right) + \frac{1}{2}\|R^n\|^2.\end{aligned} \tag{68}$$

By performing algebraic simplification on the above expression, we obtain

$$\frac{\left\|\mathrm{e}^{n+1}\right\|_H^2 - \|e^n\|_H^2}{\tau} \leq C\left(\left\|e^{n+1}\right\|_H^2 + \|e^n\|_H^2\right) + \|R^n\|, \tag{69}$$

i.e.

$$(1 - C\tau) \cdot \left\|e^{n+1}\right\|_H^2 \leq (1 + C\tau)\|e^n\|_H^2 + \tau\|R^n\|. \tag{70}$$

When τ is sufficiently small, there exists

$$\left\|e^{n+1}\right\|_H^2 \leq (HC_0\tau) \cdot \|e^n\|_H^2 + C_0\tau\|R^n\|^2, \tag{71}$$

by Grönwall's inequality, which leads us to conclude that

$$\|e^n\|_H^2 \leq e^{C_0T} \cdot \sum_{k=0}^{n-1} \tau\left\|R^k\right\|^2 \leq e^{C_0T} \cdot T \cdot \max_k \left\|R^k\right\|^2, \tag{72}$$

taking the square root of both sides results in the error estimate

$$\|e^n\|_H \leq C \max_k \left\|R^k\right\|. \tag{73}$$

Substituting this into the definition of truncation error R^n yields

$$\|e^n\|_H \leq C\left(\tau^2 + h^4\right). \tag{74}$$

This proof is completed. □

Theorem 9. *Let $e_R^n = U^n - \widehat{u}^n(\tau)$, where U^n is the exact solution and $\widehat{u}^n(\tau)$ is the numerical solution of the HOC-44 scheme. For any fixed $T > 0$, there exists a constant C independent of τ and h, such that $\|e_R^n\| \leq C\left(\tau^4 + h^4\right)$ for sufficiently small τ and h.*

Proof. Given that

$$\begin{aligned}
&U^n - u^n(\tau) = C_2\tau^2 + O\left(\tau^4\right) + O\left(h^4\right), \\
&U^n - u^{2n}\left(\frac{\tau}{2}\right) = C_2\left(\frac{\tau}{2}\right)^2 + O\left(\tau^4\right) + O\left(h^4\right) = \frac{1}{4}C_2\tau^2 + O\left(\tau^4\right) + O\left(h^4\right), \\
&U^n - u^{4n}\left(\frac{\tau}{4}\right) = C_2\left(\frac{\tau}{4}\right)^2 + O\left(\tau^4\right) + O\left(h^4\right) = \frac{1}{16}C_2\tau^2 + O\left(\tau^4\right) + O\left(h^4\right),
\end{aligned} \tag{75}$$

and further

$$\begin{aligned}
e_R^n &= U^n - \widehat{u}^n(\tau) \\
&= U^n - \left[\frac{32}{21}u^{4n}\left(\frac{\tau}{4}\right) - \frac{12}{21}u^{2n}\left(\frac{\tau}{2}\right) + \frac{1}{21}u^n(\tau)\right] \\
&= \frac{32}{21}\left[U^n - u^{4n}\left(\frac{\tau}{4}\right)\right] - \frac{12}{21}\left[U^n - u^{2n}\left(\frac{\tau}{2}\right)\right]\frac{1}{21}\left[U^n - u^n(\tau)\right] \\
&= \frac{32}{21} \cdot \frac{1}{16}C_2\tau^2 - \frac{12}{21} \cdot \frac{1}{4}C_2\tau^2 + \frac{1}{21} \cdot C_2\tau^2 + O(\tau^4) + O(h^4) \\
&= O\left(\tau^4 + h^4\right).
\end{aligned} \tag{76}$$

Therefore, $\|e_R^n\| \leq C\left(\tau^4 + h^4\right)$.

This proof is completed. □

4. Numerical Experiments

In this section, the effectiveness and accuracy of the proposed numerical schemes for the Rosenau-KdV-RLW equation, Rosenau-KdV equation, and Rosenau-RLW equation are assessed via an array of numerical experiments. All the calculations were carried out on a computer equipped with a mobile processor of the 11th generation Intel Core series using Fortran programs. The L_∞ and L_2 norm errors are defined as follows:

$$L_2 = \sqrt{h \sum_{i=1}^{N-1} (U_i - u_i)^2}, \qquad L_\infty = \max_i |U_i - u_i| .$$

The method for calculating the convergence rates of space and time is as follows:

$$\text{Rate}\,(h) = \frac{\ln(\text{error}(h_1)/\text{error}(h_2))}{\ln(h_1/h_2)}, \qquad \text{Rate}\,(\tau) = \frac{\ln(\text{error}(\tau_1)/\text{error}(\tau_2))}{\ln(\tau_1/\tau_2)},$$

where error(h_1) and error(h_2) denote the L_∞ norm errors corresponding to grid sizes h_1 and h_2, respectively. Meanwhile, error(τ_1) and error(τ_2) represent the respective errors associated with grid sizes τ_1 and τ_2 .

4.1. Rosenau-KdV-RLW Equation

4.1.1. Example 1: Solitary Wave

We consider the Rosenau-KdV-RLW Eq. (1) when the parameters $\delta = -1$, $\nu = 1$, $\alpha = 1$, $\theta = 1$, $\varepsilon = \frac{1}{2}$, $p = 2$ are taken. The computational domain is $\overline{\Omega} = [-40, 60]$, $t \in [0, T]$. The solitary wave solution is given by $u(x,t) = M\,\text{sech}^{\frac{4}{p-1}}\left[W(x - Vt)\right]$. The wave width is given by $W = \frac{p-1}{p+1}\sqrt{\frac{S-(p^2+2p+5)\alpha\nu}{32\theta\nu}}$, the wave speed is $V = \frac{\theta(p-1)^2}{(p-1)^2\delta+4\nu W^2(p^2+2p+5)}$, the amplitude is $M = \left[\frac{8(p+1)(p+3)(3p+1)\theta\nu W^4}{\varepsilon(p-1)^2(p-1)^2\delta+4(p^2+2p+5)\nu W^2}\right]^{\frac{1}{p-1}}$, where $S = \sqrt{\alpha^2\nu^2(p^2+2p+5)^2 + 16(p+1)^2\theta\nu(\theta - \alpha\delta)}$, and the initial conditions is $u(x,0) = M\,\text{sech}^{\frac{4}{p-1}}(Wx)$.

Table 1: Comparison of the convergence rate and L_∞ norm error for Example 1 at $T = 10$.

	Ref. [1]($\tau = h$)		Ref. [2]($\tau = h$)		HOC-44($\tau = h$)		HOC-24($\tau = h^2$)	
h	L_∞	$Rate(h)$	L_∞	$Rate(h)$	L_∞	$Rate(h)$	L_∞	$Rate(h)$
1	–	–	–	–	$4.2139e-04$	–	$4.8259e-01$	–
0.8	–	–	–	–	$1.2063e-04$	5.61	$2.1133e-01$	3.70
0.5	–	–	–	–	$1.2639e-05$	4.80	$3.4445e-02$	3.86
0.4	$4.6787e-04$	–	$5.4870e-02$	–	$6.0302e-06$	3.32	$1.4011e-02$	4.03
0.2	$2.9429e-05$	3.99	$7.6075e-03$	2.85	$4.4481e-07$	3.76	$8.7818e-04$	4.00

Table 2: Comparison of convergence rate, L_2 norm error and L_∞ norm error for Example 1 with $T = 10$ and $h = 0.25$.

	HOC-44				HOC-24			
τ	L_∞	$Rate(\tau)$	L_2	$Rate(\tau)$	L_∞	$Rate(\tau)$	L_2	$Rate(\tau)$
2	$5.8262e-03$	–	$1.3655e-02$	–	–	–	–	–
1	$9.0869e-04$	2.68	$2.0387e-03$	2.74	$4.9104e-01$	–	$1.1914-00$	–
1/2	$6.8152e-05$	3.74	$1.5355e-04$	3.73	$1.3500e-01$	1.15	$3.2208e-01$	2.57
1/3	$1.1002e-05$	4.50	$2.4302e-05$	4.55	$6.0857e-02$	1.97	$1.4472e-01$	1.97

Table 3: Comparison of L_∞ norm errors for Example 1 with $T = 10$ and $\tau = h$.

(h, τ)	$(0.4, 0.4)$	$(0.2, 0.2)$
Ref. [1]	$4.6787e-04$	$2.9429e-05$
Ref. [2]	$5.4870e-02$	$7.6075e-03$
HOC-24	$8.5529e-02$	$2.1788e-02$
HOC-44	$6.0302e-06$	$4.4481e-07$

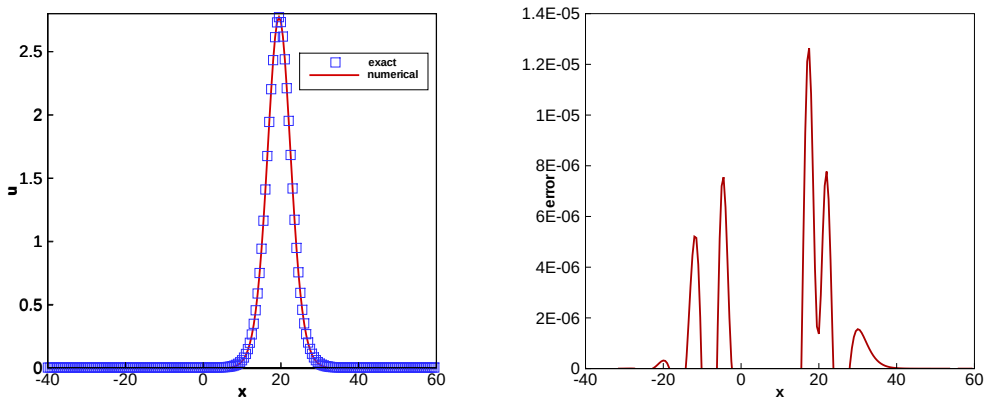
Tables 1 and 2 present the computational errors and convergence orders of the HOC-24 and HOC-44 schemes at $T = 10$. It can be observed from the tables that the HOC-24 scheme achieves fourth-order accuracy in space and second-order accuracy in time, whereas the HOC-44 scheme exhibits fourth-order accuracy in both space and time. By comparing the results in Tables 1 and 3 with those reported in Refs. [2] and [1], it is evident that the HOC-44 scheme proposed in this study offers a significant improvement in accuracy.

Table 4: The L_∞ norm error, convergence rate, and total number of time steps for Example 1 with $T = 10$.

	HOC-24($\tau = h$)			HOC-24($\tau = h^2$)			HOC-44($\tau = h$)		
h	L_∞	$Rate(h)$	M	L_∞	$Rate(h)$	M	L_∞	$Rate(h)$	M
1	$4.5737e-01$	–	10	$4.8259e-01$	–	10	$4.2139e-04$	–	10
0.8	$3.0840e-01$	1.77	12	$2.1133e-01$	3.70	15	$1.2063e-04$	5.61	12
0.5	$1.3168e-01$	1.81	20	$3.4445e-02$	3.86	40	$1.2639e-05$	4.80	20
0.4	$8.5529e-02$	1.93	25	$1.4011e-02$	4.03	62	$6.0302e-06$	3.32	25
0.2	$2.1788e-02$	1.29	50	$8.7818e-04$	4.00	250	$4.4481e-07$	3.67	50

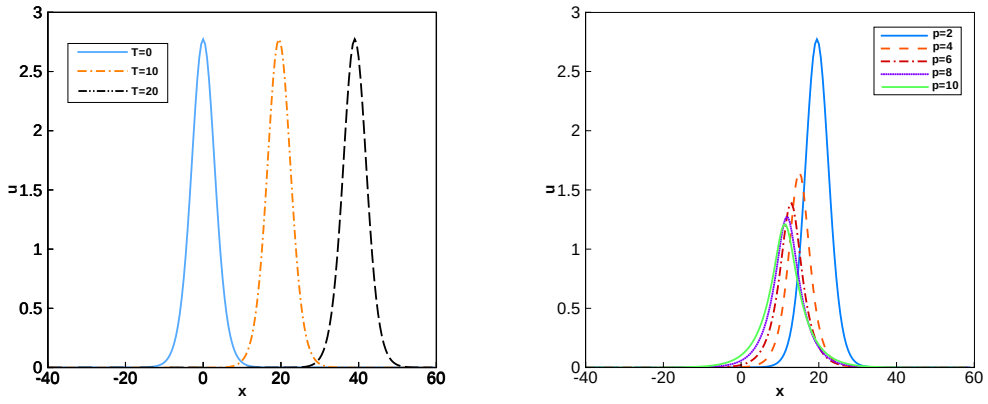
Furthermore, the results in the Tables 4 indicate that, due to a mismatch in spatio-temporal accuracy, the HOC-24 scheme requires a finer time step to fully realize its spatial accuracy. In contrast, the HOC-44 scheme demonstrates clear computational advantages at larger time step sizes. Moreover, even when applied

on fine grids, the HOC-24 scheme does not achieve the same level of accuracy as the HOC-44 scheme on coarse grids.



(a) (b)

Figure 1: (a) Numerical solution and analytical solution (b) absolute error obtained by the HOC-44 scheme with $\tau = h = 0.5$ and $T = 10$ for Example 1.



(a) (b)

Figure 2: Numerical solution obtained by the HOC-44 scheme (a) with $\tau = h = 0.5$ and $T = 0,\ 10,\ 20$ (b)with $\tau = h = 0.5$, $T = 10$ and $p = 2,\ 4,\ 6,\ 8,\ 10$ for Example 1.

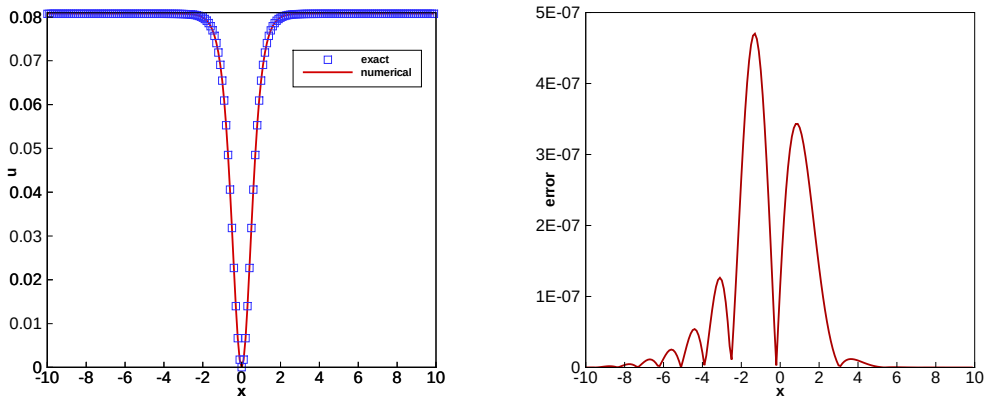
Figure 1 presents the numerical solution obtained in the HOC-44 format, the corresponding error distribution, and the analytical solution of the problem. It can be observed from the figure that the numerical solution is in high agreement with the analytical solution. Figure 2 (a) shows the evolution forms of solitary

waves at different times. It can be seen that the waveforms remain highly stable, indicating that the HOC-44 scheme has good conservation and numerical stability. Figure 2 (b) demonstrates the regulatory effect of parameter p on the shape of solitary waves: as p increases, the width of the solitary wave expands, while the amplitude of the wave crest correspondingly decreases.

4.1.2. Example 2: Shock Wave

Let Eq. (1) take the parameters $\delta = 1$, $\nu = -10$, $\alpha = 0.01$, $\theta = 0.001$, $\varepsilon = -1$, $p = 3$. The computational domain is $\overline{\Omega} = [-10, 10]$, $t \in [0, T]$. The analytical solution is $u(x,t) = M \tanh^2 [W(x - Vt)]$, the wave width is given by $W = \left[\frac{10\alpha v - \sqrt{100\alpha^2 v^2 + 46\theta\nu(\theta - \alpha\delta)}}{92\theta v}\right]^{\frac{1}{2}}$, the wave speed is $V = \frac{\alpha - 8\theta W^2}{136\nu W^4 - 8\delta W^2 + 1}$, the amplitude is $M = 2W^2\left(\frac{30V\nu}{\varepsilon}\right)^{\frac{1}{2}}$, and the initial condition is $u(x,0) = M\tanh^2(Wx)$.

Figure 3 presents the numerical solution obtained by the HOC-44 scheme for the shock problem and its corresponding analytical solution. A comparison reveals that the two are highly consistent in the position and structure of the shock, indicating that this scheme has excellent shock resolution capability and numerical stability.



(a) (b)

Figure 3: (a) Numerical solution and analytical solution (b) absolute error obtained by the HOC-44 scheme with $\tau = h = 0.1$ and $T = 10$ for Example 2.

4.2. Rosenau-KdV Equations

4.2.1. Example 3: Solitary Wave

We consider the Rosenau-KdV equation

$$\frac{\partial u(x,t)}{\partial t} + \nu \frac{\partial^5 u(x,t)}{\partial x^4 \partial t} + \alpha \frac{\partial u(x,t)}{\partial x} + \theta \frac{\partial^3 u(x,t)}{\partial x^3} + \varepsilon \frac{\partial [u(x,t)]^p}{\partial x} = 0, \ (x,t) \in \bar{\Omega} \times (0,T], \tag{77}$$

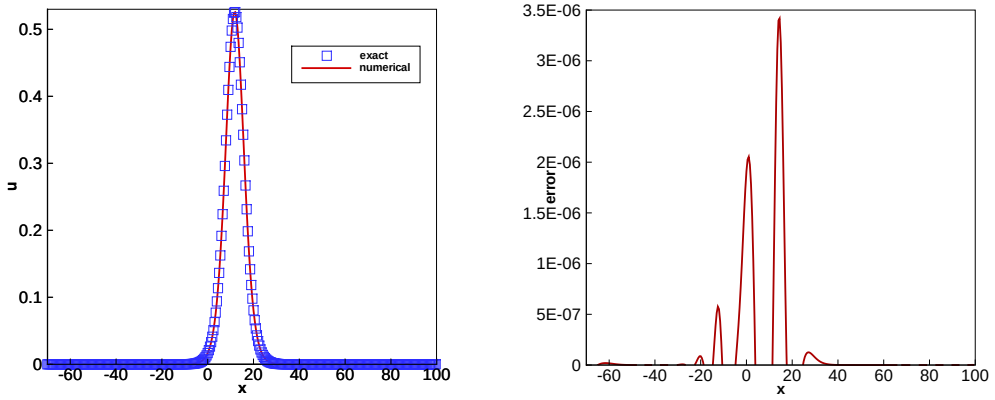
where the parameters are set as $\nu = 1$, $\alpha = 1$, $\theta = 1$, $\varepsilon = \frac{1}{2}$, $p = 2$. The computational domain is $\overline{\Omega} = [-70, 100]$. The solitary wave solution is given by $u(x,t) = M\,\mathrm{sech}^{\frac{4}{p-1}}\left[W(x - Vt)\right]$. Among these, the wave width is given by $W = \frac{p-1}{p+1}\left[\frac{-av\,(p^2+2p+5)+\sqrt{a^2v^2(p^2+2p+5)^2+16\,\theta^2 v\,(p+1)^2}}{32\,\theta\,v}\right]^{\frac{1}{2}}$, the wave speed is $V = \frac{\theta(p-1)^2}{4vW^2\,(p^2+2p+5)}$, the amplitude is $M = \left[\frac{\left[-av\,(p^2+2p+5)+\sqrt{a^2v^2(p^2+2p+5)^2+16\,\theta^2 v\,(p+1)^2}\right](p+3)\,(3p+1)}{16\,v\,\varepsilon\,(p+1)\,(p^2+2p+5)}\right]^{\frac{1}{p-1}}$, and the initial condition is $u(x,0) = M\ \mathrm{sech}^{\frac{4}{p-1}}(Wx)$.

Table 5: Comparison of convergence rate, L_2 norm error and L_∞ norm error for Example 3 at $T = 10$.

h	HOC-44($\tau = h$)				HOC-24($\tau = h^2$)			
	L_∞	$Rate(h)$	L_2	$Rate(h)$	L_∞	$Rate(h)$	L_2	$Rate(h)$
1	$6.4501e-05$	–	$1.7828e-04$	–	$1.4842e-02$	–	$3.7006e-02$	–
0.8	$2.4991e-05$	4.25	$7.0145e-05$	4.18	$6.0624e-03$	4.01	$1.5160e-02$	3.98
0.5	$3.5572e-06$	4.15	$1.0250e-05$	4.10	$9.6679e-04$	3.91	$2.3972e-03$	3.91
0.4	$1.4360e-06$	4.07	$4.1570e-06$	4.04	$3.9294e-04$	4.03	$9.7643e-04$	4.02

Table 6: Comparison of convergence rate, L_2 norm error and L_∞ norm error for Example 3 with $T = 10$ and $h = 0.25$.

τ	HOC-44				HOC-24			
	L_∞	$Rate(\tau)$	L_2	$Rate(\tau)$	L_∞	$Rate(\tau)$	L_2	$Rate(\tau)$
2	$1.1476e-04$	–	$2.8020e-04$	–	–	–	–	–
1.8	$7.4742e-05$	4.11	$1.8095e-04$	4.15	–	–	–	–
1.6	$5.1764e-05$	3.12	$1.2597e-04$	3.07	–	–	–	–
1.4	$3.2306e-05$	3.53	$7.8852e-05$	3.51	$2.7614e-02$	1.71	$6.8464e-02$	1.71
1.2	$1.7889e-05$	3.83	$4.3590e-05$	3.85	$2.0365e-02$	1.98	$5.0347e-02$	1.99
1	$9.0811e-06$	3.72	$2.2201e-05$	3.70	$1.4855e-02$	1.73	$3.6823e-02$	1.72



(a) (b)

Figure 4: (a) Numerical solution and analytical solution (b) absolute error obtained by the HOC-44 scheme with $\tau = h = 0.5$ and $T = 10$ for Example 3.

Tables 5 and 6 present the convergence orders and errors for the HOC-24 and HOC-44 schemes, respectively. The results indicate that the HOC-24 scheme achieves high spatial accuracy only when sufficiently fine time steps are employed. In contrast, the HOC-44 scheme attains comparable or higher accuracy even with larger grid step sizes. Furthermore, numerical results obtained with larger step sizes using the HOC-44 scheme exhibit greater accuracy than those produced by the HOC-24 scheme with smaller step sizes, clearly demonstrating the superiority of the high-order accurate scheme with matched spatio-temporal precision. Figure 4 shows the spatial distribution of the analytical solution of Example 3, the numerical solution obtained by the HOC-44 scheme, and the corresponding error. It can be seen that the numerical solution is in high agreement with the analytical solution, indicating that this scheme has excellent approximation capability for this problem.

Table 7: Discrete mass and discrete energy for Example 3 with $\tau = 0.1$, $h = 0.5$ and $\overline{\Omega} = [-200, 200]$.

t	HOC-44		HOC-24	
	$Q(t)$	$E(t)$	$Q(t)$	$E(t)$
0	5.498173680816660	1.989755627975355	5.498173680816660	1.989755627975355
5	5.498173680809098	1.989755628266002	5.498173680815115	1.989755648393902
10	5.498173680801313	1.989755628961163	5.498173680813657	1.989755686421391
15	5.498173680793903	1.989755629587535	5.498173680812034	1.989755724449863
20	5.498173680786084	1.989755630082744	5.498173680810672	1.989755758414401
25	5.498173680778183	1.989755630480826	5.498173680809295	1.989755787682791

Table 7 presents the results of the discrete mass and discrete energy evolution when solving Example 3 using the HOC-24 and HOC-44 schemes. The results show that both schemes strictly maintain discrete mass conservation, which is in complete agreement with the theoretical analysis. In addition, the HOC-24 scheme can strictly maintain discrete energy conservation, while the HOC-44 scheme exhibits quasi-energy conservation, and the error level of energy conservation depends on the truncation error of the scheme.

4.2.2. Example 4: Solitary Wave

We consider the Rosenau-KdV Eq. (77), where $\nu = 1$, $\alpha = 1$, $\theta = 1$, $\varepsilon = 1$, $p = 3$. The computational domain is $\overline{\Omega} = [-70, 100]$, $t \in [0, T]$. The solitary wave solution is given by $u(x,t) = k_{11}\,\mathrm{sech}^2\left[k_{12}\left(x - k_{13}t\right)\right]$. Among these, $k_{11} = \frac{1}{4}\sqrt{-15 + 3\sqrt{41}}$, $k_{12} = \frac{1}{4}\sqrt{\frac{-5+\sqrt{41}}{2}}$, $k_{13} = \frac{1}{10}\left(5 + \sqrt{41}\right)$. The initial condition is $u(x,0) = k_{11}\,\mathrm{sech}^2(k_{12}x)$.

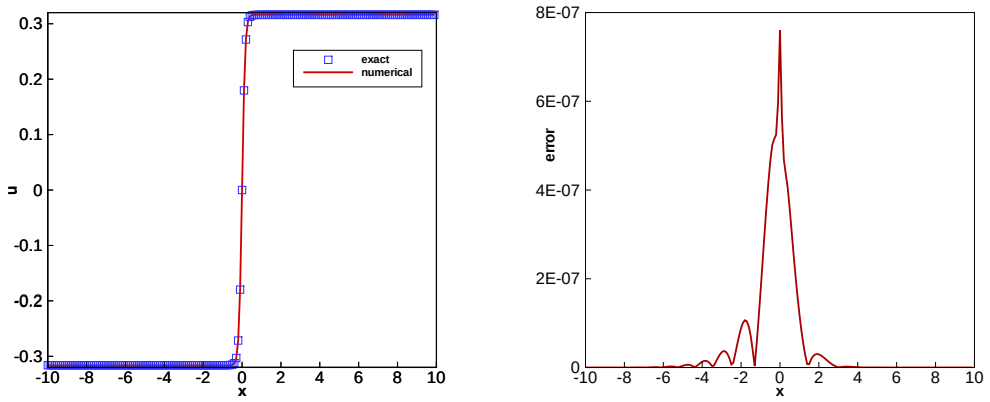
Table 8: Comparison of different methods of L_∞ norm error with $T = 40$ and $\tau = h$ for Example 4.

scheme	$h = 0.5$	$h = 0.25$
Ref. [27] ($\tau = h^2$)	–	$7.7054e-03$
Ref. [26] ($\tau = h^2$)	–	$1.3498e-02$
Ref. [24] ($\tau = h^2$)	$9.9701e-03$	$2.4561e-03$
HOC-24 ($\tau = h^2$)	$3.0972e-03$	$1.9525e-04$
HOC-44 ($\tau = h$)	$9.2346e-06$	$5.6084e-07$

Table 8 presents a comparison of the L_∞ norm errors between the HOC-24 and HOC-44 schemes discussed in this paper. It can be observed from the table that, at small time steps, the results obtained using the methods from Refs. [24, 26, 27] and the HOC-24 scheme in this study are 3 to 4 orders of magnitude larger than those achieved by the HOC-44 scheme at large time steps.

4.2.3. Example 5: Shock Wave

In this section, we consider the Rosenau-KdV Eq. (77), where $\nu = -10$, $\alpha = 0.05$, $\theta = 0.001$, $\varepsilon = -5$, $p = 5$. The computational domain is $\overline{\Omega} = [-10, 10]$, $t \in [0, T]$. The analytical solution is $u(x,t) = M\tanh\big(W(x - Vt)\big)$, the wave width is given by $W = \frac{1}{2}\left[\frac{5\alpha}{3\theta} - \frac{1}{3\theta}\sqrt{\frac{6\theta^2+25\alpha^2\nu}{\nu}}\right]^{\frac{1}{2}}$, the wave speed is $V = \frac{\alpha-2\theta W^2}{16\nu W^4+1}$, the amplitude is $M = W\left(\frac{24V\nu}{\varepsilon}\right)^{\frac{1}{4}}$, and the initial condition is $u(x,0) = M\tanh(Wx)$.



(a) (b)

Figure 5: (a) Numerical solution and analytical solution (b) absolute error by the HOC-44 scheme with $\tau = h = 0.1$ and $T = 10$ for Example 5.

Figure 5 shows the spatial distribution of the analytical solution, the numerical solution obtained by the HOC-44 scheme, and the corresponding error for Example 5. It can be seen that the numerical solution is highly consistent with the analytical solution in terms of the shock position and overall structure, indicating that the HOC-44 scheme has excellent shock resolution capability and strong discontinuity capturing performance.

4.3. Rosenau-RLW equations

Example 6 : *Solitary Wave*

We consider the Rosenau-RLW equation

$$\frac{\partial u(x,t)}{\partial t} + \delta\frac{\partial^3 u(x,t)}{\partial x^2 \partial t} + \nu\frac{\partial^5 u(x,t)}{\partial x^4 \partial t} + \alpha\frac{\partial u(x,t)}{\partial x} + \varepsilon\frac{\partial\left[u(x,t)\right]^p}{\partial x} = 0\ ,\ (x,t) \in \bar{\Omega} \times (0,T],$$

where $\delta = -1$, $\nu = 1$, $\alpha = 1$, $\varepsilon = \frac{1}{2}, p = 2$. The computational domain is $\overline{\Omega} = [-50, 150]$, $t \in [0, T]$. The solitary wave solution is given by $u(x,t) = \frac{15}{19}\mathrm{sech}^4\left[\frac{\sqrt{13}}{26}\left(x - \frac{169}{133}t\right)\right]$. The initial conditions is $u(x,0) = \frac{15}{19}\,\mathrm{sech}^4\left(\frac{\sqrt{13}}{26}x\right)$.

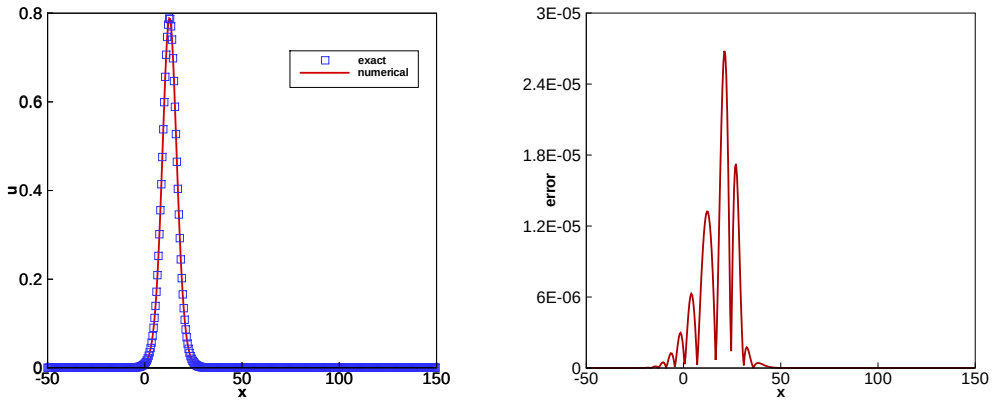
Table 9: Comparison of the convergence rate, L_2 norm error and L_∞ norm error for Example 6 at $T = 10$.

h	HOC-44($\tau = h$)				HOC-24($\tau = h^2$)			
	L_∞	$Rate(h)$	L_2	$Rate(h)$	L_∞	$Rate(h)$	L_2	$Rate(h)$
1	$2.7924e-04$	–	$6.5624e-04$	–	$3.4973e-02$	–	$8.3158e-02$	–
0.8	$1.0891e-04$	4.21	$2.5410e-04$	4.25	$1.4452e-02$	3.96	$3.3975e-02$	4.01
0.5	$1.6398e-05$	4.03	$3.8627e-05$	4.00	$2.3215e-03$	3.89	$5.4704e-03$	3.89
0.4	$6.6880e-06$	4.02	$1.5706e-05$	4.03	$9.4651e-04$	4.02	$2.2302e-03$	4.02
0.2	$3.7723e-07$	4.15	$1.1171e-06$	3.81	$5.9449e-05$	3.99	$1.4005e-04$	3.99

Tables 9 and 10 respectively present the convergence orders and corresponding error values of the HOC-24 and HOC-44 numerical formats. The computational results indicate that the HOC-24 format requires a sufficiently small time step to achieve a high spatial accuracy. In contrast, the HOC-44 format can maintain comparable or even higher computational accuracy even at a coarser grid resolution. Moreover, the numerical solutions obtained using the HOC-44 format with a larger step size are more accurate than those obtained using the HOC-24 format with a smaller step size. This fully demonstrates the advantages of the spatio-temporal consistent high-order scheme.

Table 10: Comparison of the convergence rate, L_2 norm error and L_∞ norm error for Example 6 with $T = 10$ and $h = 0.25$.

τ	HOC-44				HOC-24			
	L_∞	$Rate(\tau)$	L_2	$Rate(\tau)$	L_∞	$Rate(\tau)$	L_2	$Rate(\tau)$
2	$3.2838e-04$	–	$7.5696e-04$	–	$1.1895e-01$	–	$2.8624e-01$	–
1.8	$2.2139e-04$	3.74	$5.0425e-04$	3.86	$9.2898e-02$	2.35	$2.1969e-01$	2.51
1.6	$1.5659e-04$	2.94	$3.5877e-04$	2.89	$7.9526e-02$	1.32	$1.8905e-01$	1.28
1.4	$9.9797e-05$	3.37	$2.2909e-04$	3.36	$6.3802e-02$	1.65	$1.5156e-01$	1.65
1.2	$5.6310e-05$	3.71	$1.2895e-04$	3.73	$4.7541e-02$	1.91	$1.1232e-01$	1.94
1	$2.8809e-05$	3.68	$6.6323e-05$	3.65	$3.4855e-02$	1.70	$8.2569e-02$	1.69



(a) (b)

Figure 6: (a) Numerical solution and analytical solution (b) absolute error by the HOC-44 scheme with $\tau = h = 0.5$ and $T = 10$ for Example 6.

Figure 6 presents the spatial distribution of the analytical solution of Example 6, the numerical solution obtained by the HOC-44 scheme, and the corresponding error. It can be seen that the numerical solution is highly consistent with the analytical solution in terms of waveform structure, propagation speed, and attenuation characteristics, indicating that the HOC-44 scheme has good adaptability and high-fidelity simulation capability for the Rosenau-RLW equation.

5. Conclusions

This paper proposes a compact finite difference scheme (HOC-44) with fourth-order accuracy in both time and space for the generalized Rosenau-KdV-RLW equation, which features strong nonlinearity and high-order dispersion terms. This method aims to address the issue of low computational efficiency caused by the mismatch of temporal and spatial convergence orders in traditional numerical schemes. The main contributions and innovations of this paper are summarized as follows: (1) We employ fourth-order Pad?? approximation, fourth-order explicit compact combined operators, and fourth-order compact finite difference operators to discretize the spatial derivative terms, and adopt the Crank-Nicolson scheme combined with Richardson extrapolation in time. This strategy successfully upgrades the original HOC-24 scheme, which is second-order in time and fourth-order in space, to a fourth-order HOC-44 scheme that is consistent in both time and space. This format maintains compactness, with spatial discretization relying on only five grid points, significantly reducing storage requirements. (2) Theoretical analysis strictly proves that both the HOC-24 and HOC-44 schemes satisfy the discrete mass conservation law, and the HOC-24 scheme also

satisfies the discrete energy conservation law. The existence of the solution of the difference scheme is proved using the Brouwer fixed point theorem, and the uniqueness of the solution under certain conditions is also demonstrated. Additionally, based on the energy analysis method, we analyze the convergence and stability of the HOC-24 and HOC-44 schemes, establishing the theoretical foundation of the algorithm. (3) Through extensive numerical experiments on the evolution of solitary waves and shock waves for the Rosenau-KdV-RLW, Rosenau-KdV, and Rosenau-RLW equations, the effectiveness of the proposed scheme is verified. The numerical results show that the HOC-44 scheme can obtain more accurate numerical solutions than the HOC-24 scheme and other high-order schemes in existing literature with coarser grids and larger time steps. Moreover, the scheme exhibits excellent numerical stability in long-time simulations and can effectively capture the fine structures of large gradient solutions such as shock waves without generating non-physical oscillations. In summary, the HOC-44 scheme is a high-precision, conservative, and efficient numerical tool for solving the generalized Rosenau-KdV-RLW equation. Future work will focus on extending this compact difference strategy to high-dimensional nonlinear evolution equations in two and three dimensions and exploring its application in complex models with variable coefficients.

Data availability

The datasets used and/or analysed during the current study available from the corresponding author on reasonable request.

References

References

[1] M. Ahmat, J. Qiu, Compact ETDRK scheme for nonlinear dispersive wave equations, *Comput. Appl. Math.* 40 (8) (2021) 286.

[2] M. Ahmat, J. Qiu, SSP IMEX Runge-Kutta WENO scheme for generalized Rosenau-KdV-RLW equation, *J. Math. Study* 55 (1) (2022) 1–21.

[3] T. Ak, S.B.G. Karakoc, H. Triki, Numerical simulation for treatment of dispersive shallow water waves with Rosenau-KdV equation, *Eur. Phys. J. Plus* 131 (10) (2016) 356.

[4] A. Apolinar-Fern??ndez, J.I. Ramos, Numerical solution of the generalized, dissipative KdV-RLW-Rosenau equation with a compact method, *Commun. Nonlinear Sci. Numer. Simul.* 60 (2018) 165–183.

[5] A.R. Bahadır, Exponential finite-difference method applied to Korteweg-de Vries equation for small times, *Appl. Math. Comput.* 166 (3) (2005) 675–682.

[6] Y.F. Cui, D.K. Mao, Numerical method satisfying the first two conservation laws for the Korteweg-de Vries equation, *J. Comput. Phys.* 227 (1) (2007) 376–399.

[7] A. Esfahani, Solitary wave solutions for generalized Rosenau-KdV equation, *Commun. Theor. Phys.* 55 (3) (2011) 396–398.

[8] A. Ghiloufi, K. Omrani, New conservative difference schemes with fourth-order accuracy for some model equation for nonlinear dispersive waves, *Numer. Methods Partial Differ. Equ.* 34 (3) (2018) 835–863.

[9] J.S. Hu, Y.C. Xu, B. Hu, Conservative linear difference scheme for Rosenau-KdV equation, *Adv. Math. Phys.* 2013 (2013) 423718.

[10] M. Karta, S. Kutluay, N.M. Yagmurlu, Operator time-splitting techniques combined with quintic B-spline collocation method for the generalized Rosenau-KdV equation, *Numer. Methods Partial Differ. Equ.* 35 (1) (2019) 381–395.

[11] D.J. Korteweg, G. de Vries, On the change of form of long waves advancing in a rectangular canal, and on a new type of long stationary waves, *Philos. Mag.* 39 (240) (1895) 422–443.

[12] S. Özer, An effective numerical technique for the Rosenau-KdV-RLW equation, *BAUN Inst. Sci. Technol. J.* 20 (2) (2018) 340–353.

[13] S. Özer, Numerical solution of the Rosenau-KdV-RLW equation by operator splitting techniques based on B-spline collocation method, *Numer. Methods Partial Differ. Equ.* 35 (1) (2019) 365–380.

[14] X.T. Pan, K.L. Zheng, Numerical simulation for general Rosenau-RLW equation: an average linearized conservative scheme, *Math. Probl. Eng.* 2012 (2012) 517818.

[15] X.T. Pan, K.L. Zheng, On the convergence of a conservative numerical scheme for the usual Rosenau-RLW equation, *Appl. Math. Model.* 36 (8) (2012) 3371–3378.

[16] X.T. Pan, K.L. Zheng, L.M. Zhang, Finite difference discretization of the Rosenau-RLW equation, *Appl. Anal.* 92 (12) (2013) 2590–2601.

[17] D.H. Peregrine, Calculations of the development of an undular bore, *J. Fluid Mech.* 25 (2) (1966) 321–330.

[18] D.H. Peregrine, Long waves on a beach, *J. Fluid Mech.* 27 (4) (1967) 815–827.

[19] P. Razborova, H. Triki, A. Biswas, Perturbation of dispersive shallow water waves, *Ocean Eng.* 63 (2013) 1–7.

[20] P. Rosenau, A quasi-continuous description of a nonlinear transmission line, *Phys. Scr.* 34 (6) (1986) 827–829.

[21] P. Rosenau, Dynamics of dense discrete systems–high order effects, *Prog. Theor. Phys.* 79 (5) (1988) 1028–1042.

[22] Shallu, V.K. Kukreja, An efficient collocation algorithm with SSP-RK43 scheme to solve Rosenau-KdV-RLW equation, *Int. J. Appl. Comput. Math.* 7 (5) (2021) 161.

[23] B. Wang, T.J. Sun, D. Liang, The conservative and fourth-order compact finite difference schemes for regularized long wave equation, *J. Comput. Appl. Math.* 356 (2019) 244–263.

[24] X. Wang, W. Dai, A conservative fourth-order stable finite difference scheme for the generalized Rosenau-KdV equation in both 1D and 2D, *J. Comput. Appl. Math.* 356 (2019) 310–331.

[25] X. Wang, W. Dai, A new conservative finite difference scheme for the generalized Rosenau-KdV-RLW equation, *Comput. Appl. Math.* 39 (3) (2020) 237.

[26] M. Zheng, J. Zhou, An average linear difference scheme for the generalized Rosenau-KdV equation, *J. Appl. Math.* 2014 (2014) 202793.

[27] J. Zhou, M. Zheng, X. Da, Study on convergence and stability of a conservative difference scheme for the generalized Rosenau-KdV equation, *J. Nonlinear Sci. Appl.* 10 (5) (2017) 2735–2742.

[28] J. Zhou, M. Zheng, R.X. Jiang, The conservative difference scheme for the generalized Rosenau-KdV equation, *Therm. Sci.* 20 (3) (2016) 903–910.

[29] J.M. Zuo, Solitons and periodic solutions for the Rosenau-KdV and Rosenau-Kawahara equations, *Appl. Math. Comput.* 215 (2) (2009) 835–840.

Acknowledgements

We sincerely thank the editorial team and anonymous reviewers of Scientific Reports for their valuable feedback and thoughtful suggestions, which significantly improved the quality of this work.

Funding

This work is partially supported by the Foreign Expert Program (G2023045002L), Natural Science Foundation of Ningxia (2025AAC030584), the Key Research and Development Program of Ningxia(2021BEB04053), Research Startup Funding for Full-time High-level Talents Introduced by Ningxia Hui Autonomous Region (2024BEH04096),the Special Project for Talent Introduction under the Autonomous Region's Key Research and Development Program (2025BEH04100), the Ningxia Normal University School-level Scientific Research Project Funding (NSDXJGR02), the Ningxia Overseas Talent Introduction Project, the Ningxia Youth Science and Technology Support Program, the Research Platform of the Artificial Intelligence and Intelligent Medical Engineering Technology Research Center of Ningxia Normal University and Plan for Introducing

Foreign Talents in Ningxia.

Competing interests

Conflict of Interest: The authors declare that they have no competing interests related to the content of this article.